Spectral Properties of Local Field Potentials and Electroencephalograms as Indices for Changes in Neural Circuit Parameters

Pablo Martínez-Cañada[1,2(✉)] and Stefano Panzeri[1,3]

[1] Neural Computation Laboratory, Center for Neuroscience and Cognitive Systems, Istituto Italiano di Tecnologia, Genova and Rovereto, Italy
`pablo.martinez@iit.it`
[2] Optical Approaches to Brain Function Laboratory, Istituto Italiano di Tecnologia, Genova, Italy
[3] Department of Neural Information Processing, Center for Molecular Neurobiology (ZMNH), University Medical Center Hamburg-Eppendorf (UKE), Hamburg, Germany
`stefano.panzeri@zmnh.uni-hamburg.de`

Abstract. Electrical measurements of aggregate neural activity, such as local field potentials (LFPs) or electroencephalograms (EEGs), can capture oscillations of neural activity over a wide range of frequencies and are widely used to study brain function and dysfunction. However, relatively little is known about how to relate features of such aggregate neural recordings to the functional and anatomical configurations of the underlying neural circuits that produce them. An important neural circuit parameter which has profound effects on neural network dynamics and neural function is the ratio between excitation and inhibition (E:I), which has been found to be atypical in many neuropsychiatric conditions. Here we used simulations of recurrent networks of point-like leaky integrate-and-fire (LIF) neurons to study how to infer parameters such as the E:I ratio or the magnitude of the external input of the network from aggregate electrical measures. We used approximations (or proxies), validated in previous work, to generate realistic LFPs and EEGs from simulations of such networks. We computed different spectral features from simulated neural mass signals, such as the 1/f spectral power law or the Hurst exponent (H), and studied how these features changed when we changed the E:I ratio or the strength of the external input of the network model. We discuss how different spectral features of aggregate signals relate to the E:I ratio or the strength of the external input and outline our efforts to fit our model, in future work, to multiple measures extracted from empirical recordings of aggregate neural activity.

1   Introduction

Electrical recordings of aggregate neural activity, such as local field potentials (LFPs) or electroencephalograms (EEGs), have been a mainstream technique for studying large-scale brain dynamics, with important applications for both scientific research [5,10,13,19] and clinical diagnosis [2,3,21,24]. These recordings have been shown to capture how oscillatory aspects of neural activity change, over a wide range of frequencies, with cognitive or sensory tasks or in brain dysfunction [6,8,10,12]. Aggregate neural signals conflate different neural processes within and among different classes of cells and different spatial locations. This makes them difficult to interpret in terms of contributions of the different underlying neural phenomena. Determining the individual neural mechanisms that give rise to the different features of LFPs and EEGs, and quantifying how these features change with manipulations of neural circuits or in brain disorders, would significantly enhance our ability to understand the brain. Yet, how to accomplish this remains a major and largely unaddressed challenge.

An important parameter that describes local neural circuit dynamics is the excitation and inhibition (E:I) ratio. This ratio has been theorized to be a potential biomarker of many medical conditions, including autism [20,22]. Neural network models [4,11] have demonstrated that changes in the E:I ratio of the network have a direct effect on the spectral shape of neural activity, which suggests that features of power spectra of neural time-series data could be used to predict the E:I ratio. In previous work [23], we investigated different measures computed on the power spectrum of LFPs and blood oxygen level dependent (BOLD) signal that could be used to reliably estimate the E:I ratio: the exponent of the 1/f spectral power law, slopes for the low- and high-frequency regions of the spectrum and the Hurst exponent (H). We simulated the LFP and BOLD signal from our recurrent network model [7,15,17,18] of leaky integrate-and-fire (LIF) neuronal populations, and studied how these spectral measures changed when we manipulated the E:I ratio by independently varying the strengths of the inhibitory (g_I) and excitatory (g_E) synaptic conductances.

In this paper we take steps forward from our prior work [23] and present new results in the following directions. First, we used more realistic models to generate neural mass signals. In previous work [23], we computed the network's LFP as the sum of absolute values of synaptic currents. This is a simple and reasonable approximation (or proxy), which has been shown to work fairly well in describing both real cortical data [1,15,17] and field potentials and EEGs generated by simulations with networks of realistically-shaped 3D neurons [14, 16]. However, our recent work has demonstrated that it is possible to obtain better approximations of the LFP/EEG from networks of point neurons [14,16]. Second, in addition to previous spectral measures based on frequency slopes or H, here we analyze other metrics of power spectra to perform a systematic study

of how different spectral features may contribute to the underlying changes in neural network parameters. We thus investigated how frequency slopes, H and other spectral properties (e.g., gamma peak frequency and gamma band power) of the different proxies change as a function of the ratio between inhibitory and excitatory conductances ($g = g_I/g_E$). Consistent with previous results [4, 17], we increased the firing rate of the external input of the network model to produce stronger and faster gamma oscillations in the proxy power spectra and we evaluated how these spectral measures are affected by this oscillatory activity. This led us to identify complementary ways in which different spectral features of aggregate neural signals encode changes in the network parameters.

Based on these encouraging results, in the Discussion, we pursue the idea that a suitable combination of spectral properties of LFPs/EEGs could be used to isolate such biomarkers of E:I ratio in power spectrum curves that have both 1/f aperiodic and periodic components.

2   Results

2.1   Simulation of Power Spectra of Neural Mass Signals from a Recurrent Network Model

As described in previous work [7,14,15,17,23], we used a network model of excitatory and inhibitory LIF neurons recurrently connected to simulate realistic cortical dynamics. The network was composed of 5000 neurons: 4000 were excitatory and 1000 inhibitory. The neurons were randomly connected with a connection probability between each pair of neurons of 0.2. This means that, on average, the number of incoming excitatory and inhibitory connections onto each neuron was 800 and 200, respectively. The network receives external synaptic input that carries sensory information and stimulus-unrelated inputs representing slow ongoing fluctuations of cortical activity.

From simulation of the point-like neuron network model, we computed different approximations (termed proxies) of aggregate electrical signal based on a weighted sum of synaptic currents. The first proxy is the average sum of absolute values of all synaptic currents ($\sum |I|$). The second proxy is a parametrized linear combination of AMPA and GABA currents that was found to perform well in approximating the LFP [16]: the LFP reference weighted sum (LRWS). We also evaluated a new class of current-based proxies whose parameters were optimized to fit the EEG across different network states of the point-neuron network [14]: the EEG reference weighted sum 1 (ERWS1) and the EEG reference weighted sum 2 (ERWS2). The difference between ERWS1 and ERSW2 is that parameters of ERWS2 adapt theirs values as a function of the strength of the external input ν_0, whereas the parameters of ERWS1 are not dependent on ν_0.

We then generated a large set of numerical simulations by systematically varying two parameters of the network model that are of interest to our study: the ratio between inhibitory and excitatory conductances ($g = g_I/g_E$), which is hypothesized to be related to the E:I ratio in the brain, and the firing rate ν_0 of the external input, which can elicit entrainment of gamma oscillations in the model.

For each simulation, we computed the power spectral density (PSD) functions of all the proxies and their spectral features were parametrized in the (1–150) Hz frequency range by two fitting algorithms. The first one is the FOOOF algorithm [9], which automatically splits neural PSDs into 1/f aperiodic and periodic (oscillatory) components. Parameters of the FOOOF algorithm were selected as follows. Maximum number of peaks: 2 (ν_0 = 1.5 spikes/s), 3 (ν_0 = 2 spikes/s) and 4 (ν_0 = 3 spikes/s). Peak width limits: (5–100) Hz. Peak threshold: 2 standard deviations. We also computed the piecewise linear regression functions that fit the proxy PSDs over two different frequency ranges (with a cutoff frequency that was 30 Hz for ν_0 = 1.5 or 2 spikes/s and 40 Hz for ν_0 = 3 spikes/s).

Some example PSDs and their spectral fittings are shown in Fig. 1 for 3 levels of strength of external input ν_0 (1.5, 2 and 3 spikes/s) and 3 values of g (5.6, 11.3 and 14.8). The PSDs generated by our model exhibited both periodic and 1/f aperiodic components whose properties were modified by the choice of values of g and ν_0. For the reference value g = 11.3 [15,17], when the external rate was low (ν_0 = 1.5 spikes/s), the power spectrum was dominated by the aperiodic component that has a 1/f-like distribution, with exponentially decreasing power across increasing frequencies. An increase of ν_0 (ν_0 = 2 and 3 spikes/s) added periodic oscillatory peaks to the 1/f curve, which were more prominent in the gamma range (30–100 Hz). The dependence of the gamma oscillation on the input rate shows that, consistent with previous results [7,17], the gamma oscillation becomes stronger and faster as the input is increased.

2.2   Changes in the Ratio Between Inhibitory and Excitatory Conductances and External Input Strength Modulate Spectral Features

Changing g from the reference value shifted the network dynamics to different neural regimes, an excitation-dominated regime ($g < 11.3$) or an inhibition-dominated regime ($g > 11.3$), and modified properties of gamma oscillations. We computed from our model three measures to quantify spectral features in the gamma band: peak frequency, power modulation and peak bandwidth. We plotted them in Fig. 2 as a function of the inhibition-excitation ratio (g). Overall, a decrease of g from the reference value (that is, g is shifted in favor of excitation) produced more prominent changes in parameter values of the gamma oscillation than an increase of g. When g was decreased, we observed a decrease of the peak frequency, a weaker power modulation and a reduction of the peak bandwidth. While the peak frequency and the peak power modulation were the two metrics that produced the most similar values across proxies, the peak bandwidth values showed more variability across proxies and also over the values of g. It is important to note that the relationship between g and spectral parameters in the inhibition-dominated regime flattens out for low values of strength of external input (ν_0 = 2 spikes/s). However, an increase of the strength of external input (ν_0 = 3 spikes/s) produced variations of parameters of gamma oscillations in the inhibition-dominated regime that were sizeable.
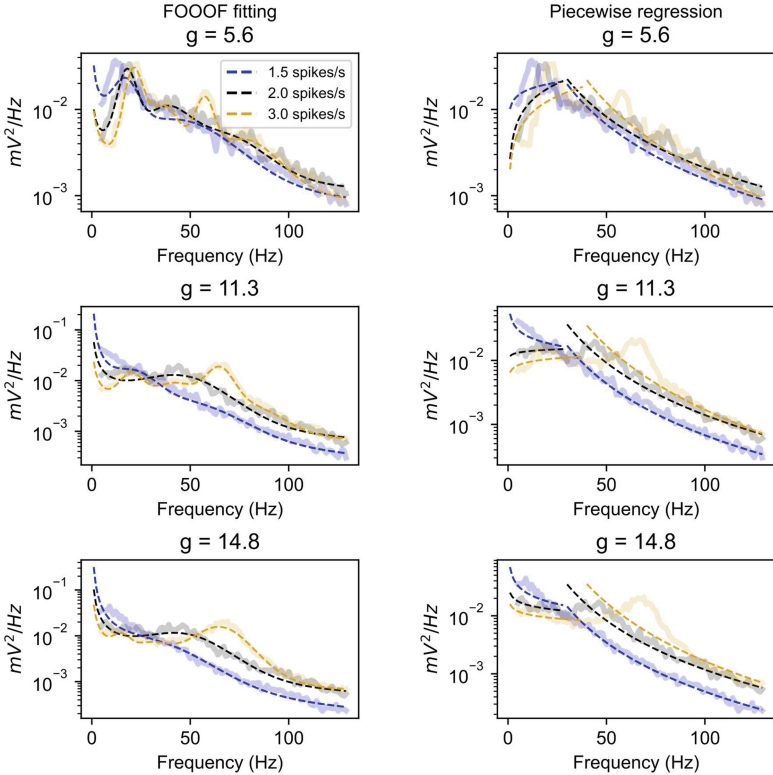
Fig. 1. Examples of proxy PSDs (solid lines) and spectral fittings (dashed lines) using the FOOOF algorithm [9] or a piecewise linear regression, plotted for 3 levels of strength of external input ν_0 (1.5, 2 and 3 spikes/s) and 3 values of g (5.6, 11.3 and 14.8). The PSDs were computed using the ERWS2 proxy.

Based on our previous work [23], we calculated slopes for the low- and high-frequency regions, slope of the $1/f$ aperiodic component generated by the FOOOF algorithm and the Hurst exponent (H) as a function of g, but here (Fig. 3) we extended our previous work by computing and comparing these spectral metrics for different proxy PSDs and for a stronger gamma oscillation ($\nu_0 = 3$ spikes/s). The different proxies produced similar values of low-frequency slopes for all rates of external input ($\nu_0 = 1.5$, 2 and 3 spikes/second). The high-frequency slope, aperiodic slope and H of the different proxies showed similar shapes as a function of g but with different offsets that depended on the external input rate. As the external input rate increased, the proxies produced values of slopes and H that were clustered in two groups: one formed by $\sum |I|$ and LRWS and the other by ERWS1 and ERWS2.

In agreement with our previous results [23], an increase in g beyond the reference value (shifting g towards stronger inhibition) had a weaker effect on slopes and H for $\nu_0 = 1.5$ or 2 spikes/s. However, when we increased the external
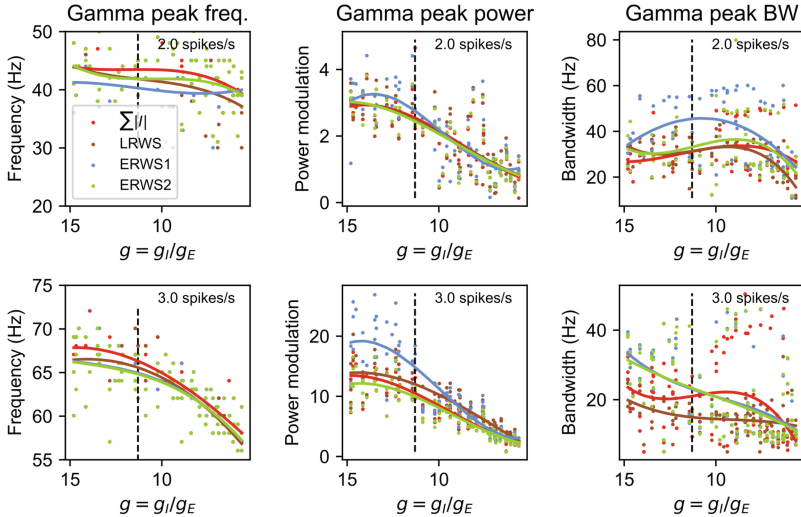
Fig. 2. Parameter values of the gamma oscillation (peak frequency, power modulation of the peak and peak bandwidth - BW) of the different proxy PSDs ($\sum|I|$, LRWS, ERWS1 and ERWS2), as a function of g for 2 levels of strength of external input ν_0 (2 and 3 spikes/s). The gamma oscillation is defined as the strongest power peak for frequencies 30 Hz ($\nu_0 = 1.5$ or 2 spikes/s) or 40 Hz ($\nu_0 = 3$ spikes/s).

input ($\nu_0 = 3$ spikes/s), we found that slopes (especially the low-frequency slope and aperiodic slope) in the inhibition-dominated regime showed changes comparable to changes in the excitation-dominated regime. Slopes in the excitation-dominated regime ($g < 11.3$) increase, that is, slopes flatten with decreasing g, although the relative amount of increase of the slopes is different depending on the value of ν_0. Analogously, H decreases with decreasing g below the baseline reference value for $\nu_0 = 1.5$ or 2 spikes/s. Changes in H as a function of g are less clear for $\nu_0 = 3$ spikes/s.

2.3 Major Limitations of the LFP and EEG Proxies

In the definition and computation of LFP and EEG proxies, we made some simplifying assumptions [14,16]. We considered a single cortical layer in the generation of LFPs/EEGs (L2/3) instead of the multi-layer structure of cortex. Although we have shown that our proxies generalize well for different L2/3 pyramidal-cell morphologies [14,16], it will be important to extend our work to quantify contributions from other cortical laminae and cell morphologies to the LFPs/EEGs. Another limitation is that our simple recurrent network model cannot produce internally generated oscillations in the canonical lower-frequency bands (delta, theta, alpha, and beta) commonly observed in EEG and MEG. The connectivity of the recurrent network model was distance-independent, which approximates the local connectivity of a cortical column. Since the EEG signal
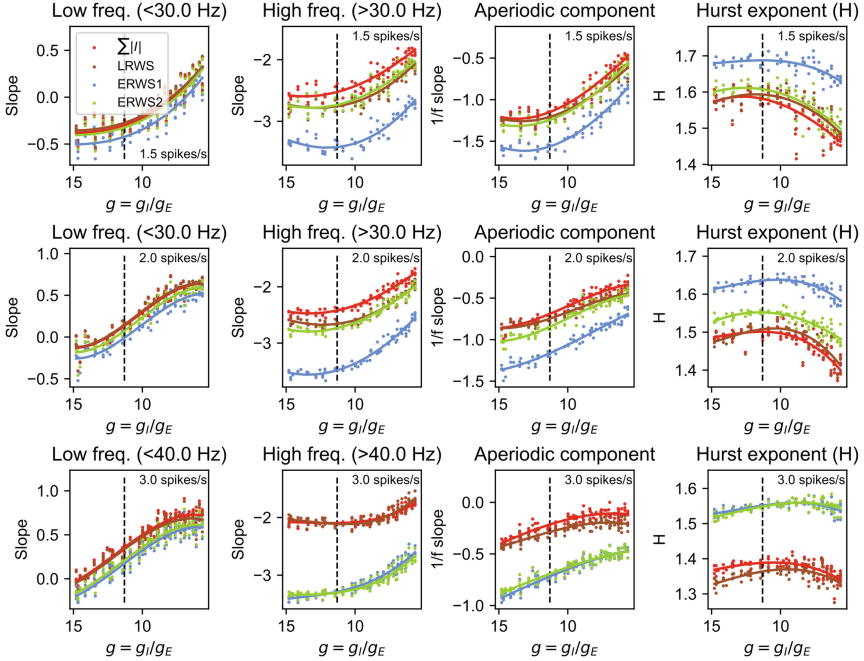
Fig. 3. Low- and high-frequency slopes, 1/f aperiodic component and H values, computed for the different proxy PSDs ($\sum |I|$, LRWS, ERWS1 and ERWS2), plotted as a function of g for three different firing rates of external input ν_0 (1.5, 2 and 3 spikes/second).

may integrate neural activity from distances typically larger than a cortical column, it will be essential to include realistic distance-dependent connectivity in future versions of the EEG proxies.

3   Discussion

In this work we explored the idea that spectral properties of neural mass signals (e.g., LFPs or EEGs) could be used to isolate key descriptors of the underlying neural circuit, such as the E:I ratio. We used a recurrent network model [7, 15,17,18] to simulate power spectra of aggregate neural signals and studied how spectral properties changed when manipulating the ratio between inhibitory and excitatory conductances ($g = g_I/g_E$). The metrics that we used are based on spectral properties commonly used in the literature to analyze the spectral shape of neural activity [9,11], such as the 1/f slope or the Hurst exponent (H). Here we have extended our previous work [23] by studying the effects of gamma oscillatory activity on these spectral metrics and by utilizing, and comparing, different proxies proposed in the literature to generate the LFP or EEG from networks of point neurons.

Prior work [11,23] suggested that an increase of the E:I ratio would produce an increase of the slope value (i.e. flatter, less negative slopes) or, analogously, a decrease of H. Results obtained with our model of recurrent excitation and inhibition are largely compatible with these studies. Additionally, in our previous work [11,23], we found that the relationship between E:I and spectral slopes flattens out for high values of I. Here we have confirmed these results for low levels of external input strength ($\nu_0 = 1.5$ or 2 spikes/s). In past work [14], we observed that for low firing rates of external input, synaptic currents of the network model, computed for the baseline regime of g ($g = 11.3$), were dominated by slow inhibitory currents, which produce a strong low-pass filtering of LFP/EEG power spectra. This suggests that a further increase of recurrent inhibition from $g = 11.3$ may not have an effective increase of the low-pass filtering effects of inhibitory currents, which could explain why slopes do not change significantly for high values of I. We then increased the firing rate of the external input ($\nu_0 = 3$ spikes/s) and found that low-frequency and aperiodic slopes in the inhibition-dominated regime exhibited changes comparable to changes in the excitation-dominated regime. As shown in results of Ref. [7], computed for the baseline regime of g ($g = 11.3$), an increase of the external input rate led to a stronger reduction of post-synaptic inhibitory currents with respect to excitatory currents. Thus, an increase of ν_0 could produce a reduction of the low-pass filtering effect of slow inhibitory currents for the baseline regime of g, resulting in flatter aperiodic slopes for $g = 11.3$ (as shown in Fig. 3, third column), and may leave room for a further reduction of the aperiodic slope for high values of I.

Taken together, our results suggest that the different metrics of neural power spectra evaluated in this work could be combined to reliably predict changes in the E:I ratio for power spectra that have different features of 1/f aperiodic and periodic components. By fitting our network model, in future work, to multiple measures extracted from empirical recordings of neural mass signals, estimates of the E:I ratio (or other key properties of the neural circuit such as the strength of the external input) could be obtained from EEG and LFP spectra or evoked potentials. This will give us the possibility to use the recurrent network model as a tool to interpret measurements of aggregate neural activity in terms of neural circuit parameters.

References

1. Barbieri, F., Mazzoni, A., Logothetis, N.K., Panzeri, S., Brunel, N.: Stimulus dependence of local field potential spectra: experiment versus theory. J. Neurosci. **34**, 14589–14605 (2014)
2. Bosl, W., Tierney, A., Tager-Flusberg, H., Nelson, C.: EEG complexity as a biomarker for autism spectrum disorder risk. BMC Med. **9**(1), 1–16 (2011)
3. Bosl, W.J., Loddenkemper, T., Nelson, C.A.: Nonlinear EEG biomarker profiles for autism and absence epilepsy. Neuropsychiatric Electrophysiol. **3**(1), 1–22 (2017)
4. Brunel, N., Wang, X.J.: What determines the frequency of fast network oscillations with irregular neural discharges? i. synaptic dynamics and excitation-inhibition balance. J. Neurophysiol. **90**(1), 415–430 (2003)

5. Buzsáki, G., Anastassiou, C.A., Koch, C.: The origin of extracellular fields and currents - EEG, ECoG. LFP and spikes. Nat. Rev. Neurosci. **13**(6), 407–420 (2012)
6. Buzsáki, G., Wang, X.J.: Mechanisms of gamma oscillations. Ann. Rev. Neurosci. **35**, 203–225 (2012)
7. Cavallari, S., Panzeri, S., Mazzoni, A.: Comparison of the dynamics of neural interactions between current-based and conductance-based integrate-and-fire recurrent networks. Front. Neural Circuits **8**, 12 (2014)
8. Colgin, L.L., et al.: Frequency of gamma oscillations routes flow of information in the hippocampus. Nature **462**(7271), 353–357 (2009)
9. Donoghue, T., et al.: Parameterizing neural power spectra into periodic and aperiodic components. Nat. Neurosci. **23**(12), 1655–1665 (2020)
10. Einevoll, G.T., Kayser, C., Logothetis, N.K., Panzeri, S.: Modelling and analysis of local field potentials for studying the function of cortical circuits. Nat. Rev. Neurosci. **14**(11), 770–785 (2013)
11. Gao, R., Peterson, E.J., Voytek, B.: Inferring synaptic excitation/inhibition balance from field potentials. Neuroimage **158**, 70–78 (2017)
12. Herrmann, C., Demiralp, T.: Human EEG gamma oscillations in neuropsychiatric disorders. Clin. Neurophysiol. **116**(12), 2719–2733 (2005)
13. Mahmud, M., Vassanelli, S.: Processing and analysis of multichannel extracellular neuronal signals: state-of-the-art and challenges. Front. Neurosci. **10**, 248 (2016)
14. Martínez-Cañada, P., Ness, T.V., Einevoll, G.T., Fellin, T., Panzeri, S.: Computation of the electroencephalogram (EEG) from network models of point neurons. PLoS Comput. Biol. **17**(4), e1008893 (2021)
15. Mazzoni, A., Brunel, N., Cavallari, S., Logothetis, N.K., Panzeri, S.: Cortical dynamics during naturalistic sensory stimulations: experiments and models. J. Physiol. Paris **105**(1), 2–15 (2011)
16. Mazzoni, A., Lindén, H., Cuntz, H., Lansner, A., Panzeri, S., Einevoll, G.T.: Computing the Local Field Potential (LFP) from integrate-and-fire network models. PLoS Comput. Biol. **11**(12), e1004584 (2015)
17. Mazzoni, A., Panzeri, S., Logothetis, N.K., Brunel, N.: Encoding of naturalistic stimuli by local field potential spectra in networks of excitatory and inhibitory neurons. PLoS Comput. Biol. **4**(12), e1000239 (2008)
18. Mazzoni, A., Whittingstall, K., Brunel, N., Logothetis, N.K., Panzeri, S.: Understanding the relationships between spike rate and delta/gamma frequency bands of LFPs and EEGs using a local cortical network model. NeuroImage **52**(3), 956–972 (2010)
19. Pesaran, B., et al.: Investigating large-scale brain dynamics using field potential recordings: analysis and interpretation. Nat. Neurosci. **21**(7), 903–919 (2018)
20. Rubenstein, J., Merzenich, M.M.: Model of autism: increased ratio of excitation/inhibition in key neural systems. Genes Brain Behav. **2**(5), 255–267 (2003)
21. da Silva, F.L.: EEG and MEG: relevance to neuroscience. Neuron **80**(5), 1112–1128 (2013)
22. Sohal, V.S., Rubenstein, J.L.: Excitation-inhibition balance as a framework for investigating mechanisms in neuropsychiatric disorders. Mol. Psychiatry **24**(9), 1248–1257 (2019)
23. Trakoshis, S., et al.: Intrinsic excitation-inhibition imbalance affects medial prefrontal cortex differently in autistic men versus women. eLife **9**, e55684 (2020)
24. Wang, J., Barstein, J., Ethridge, L.E., Mosconi, M.W., Takarae, Y., Sweeney, J.A.: Resting state EEG abnormalities in autism spectrum disorders. J. Neurodevelopmental Disord. **5**(1), 1–14 (2013)